PPD 0 and returned to the virgin control level at PPD 28 (on weaning), indicating that this biological control mechanism may also be present during lactation. Experiments remain to be performed on whether prolactin and/or oxytocin could suppress the activities of drug metabolizing enzymes and reduce CYPs protein.

Oxidative stress may be one of the factors which are responsible for the regulation of CYPs during rat lactation. Oxidative stress has been suggested to result in the reduction of total CYP450 levels and drug metabolizing activities in vivo (Mannering and Deloria, 1986; Peristeris et al., 1992; Gatti et al., 1993; Liu et al., 1993). Furthermore, Barker et al. (1994) have investigated the possibility that oxidative stress may influence inducer-dependent expression of CYP1A1 and CYP1A2 and demonstrated that hydrogen peroxide suppresses the accumulation of CYP1A1 and CYP1A2 mRNAs in isolated hepatocytes through a transcriptional mechanism. Pahan et al. (1997) demonstrated that there is a down-regulation of CYP2E1 in rat liver peroxisomes by a mechanism of ischemia/reperfusion-induced oxidative stress. Investigation by Upreti et al. (2002) indicated that significantly higher lipid peroxidation levels were established in all the major organs of rat during lactation. Furthermore, they also demonstrated that the early lactation generated higher oxidative stress compared with the late periods of lactation. This seems to be consistent with our data: six CYPs proteins were markedly decreased at PPD 0, and four of them returned to the virgin control level on PPD 14. In human, lipid peroxidation is increased during pregnancy, and delivery alone is a major source of oxidative stress (Arikan et al., 2001), probably confirming the results obtained at PPD 0 in this study. Therefore, oxidative stress may play a role in the regulation of CYPs protein during rat lactation.

Although endogenous nitric oxide (NO), a potent vasodilator and a platelet anti-aggregating factor, has been suggested to be involved in the regulation of CYPs protein during rat pregnancy (He et al., 2005), the data of changes in NO during rat lactation are absent.

Taken together, the results of the present study suggest that rat lactation is accompanied with decreases in some CYPs proteins levels. Effects of lactation on decreases in CYPs protein levels were more predominant at birth day (PPD 0) than at peak lactation (PPD 14). All the decreased CYPs proteins were at virgin control levels by 7 days post-lactation (PPD 28), clearly suggesting that biological changes during rat lactation could influence the expression of hepatic CYPs protein. Further studies are required to elucidate the mechanism of effects of lactation on down-regulation of CYPs protein.

References

Abel, E.L., Greizerstein, H.B., Siemens, A.J., 1979. Influence of lactation on rate of disappearance of ethanol in the rat. Neurobehav. Toxicol. 1, 185–186.

Arikan, S., Konukoglu, D., Arikan, C., Akcay, T., Davas, I., 2001. Lipid peroxidation and antioxidant status in maternal and cord blood. Gynecol. Obstet. Invest. 51, 145–149.

Barker, C.W., Fagan, J.B., Pasco, D.S., 1994. Down-regulation of P4501A1 and P4501A2 mRNA expression in isolated hepatocytes by oxidative stress. J. Biol. Chem. 269, 3985–3990.

Borlakoglu, J.T., Scott, A., Henderson, C.J., Wolf, C.R., 1993. Alterations in rat hepatic drug metabolism during pregnancy and lactation. Biochem. Pharmacol. 46, 29–36.

Dean, M.E., Stock, B.H., 1975. Hepatic microsomal metabolism of drugs during pregnancy in the rat. Drug Metab. Dispos. 3, 325–331.

Dean, M.E., Stock, B.H., 1989. The influence of phenobarbital administration on hepatic monooxygenase activity at various stages of gestation in the rat. Drug Metab. Dispos. 17, 579–581.

Feuer, G., 1979. Action of pregnancy and various progesterones on hepatic microsomal activities. Drug Metab. Rev. 9, 147–169.

Feuer, G., Liscio, A., 1969. Origin of delayed development of drug metabolism in the newborn rat. Nature 223, 68–70.

Gatti, S., Faggioni, R., Echtenacher, B., Ghezzi, P., 1993. Role of tumour necrosis factor and reactive oxygen intermediates in lipopolysaccharide-induced pulmonary oedema and lethality. Clin. Exp. Immunol. 91, 456–461.

Guarino, A.M., Gram, T.E., Schroeder, D.H., Call, J.B., Gillette, J.R., 1969. Alterations in kinetic constants for hepatic microsomal aniline hydroxylase and ethylmorphine *N*-demethylase associated with pregnancy in rats. J. Pharmacol. Exp. Ther. 168, 224–228.

He, X.J., Ejiri, N., Nakayama, H., Doi, K., 2005. Effects of pregnancy on CYPs protein expression in rat liver. Exp. Mol. Pathol. 78, 64–70.

Heil, S.H., Subramanian, M.G., 1998. Alcohol and the hormonal control of lactation. Alcohol Health Res. World 22, 178–184.

Lind, A.B., Wadelius, M., Darj, E., Finnstrom, N., Lundgren, S., Rane, A., 2003. Gene expression of cytochrome P450 1B1 and 2D6 in leukocytes in human pregnancy. Pharmacol. Toxicol. 92, 295–299.

Liu, P.T., Kentish, P.A., Symons, A.M., Parke, D.V., 1993. The effects of ether anaesthesia on oxidative stress in rats-dose response. Toxicology 80, 37–49.

Mannering, G.J., Deloria, L.B., 1986. The pharmacology and toxicology of the interferons: an overview. Annu. Rev. Pharmacol. Toxicol. 26, 455–515.

Neale, M.G., Parke, D.V., 1973. Effects of pregnancy on the metabolism of drugs in the rat and rabbit. Biochem. Pharmacol. 22, 1451–1461.

Pahan, K., Smith, B.T., Singh, A.K., Singh, I., 1997. Cytochrome P-450 2E1 in rat liver peroxisomes: downregulation by ischemia/reperfusion-induced oxidative stress. Free Radical Biol. Med. 23, 963–971.

Peristeris, P., Clark, B.D., Gatti, S., Faggioni, R., Mantovani, A., Mengozzi, M., Orencole, S.F., Sironi, M., Ghezzi, P., 1992. *N*-acetylcysteine and glutathione as inhibitors of tumor necrosis factor production. Cell. Immunol. 140, 390–399.

Smith, R.W., 1975. The effects of pregnancy and lactation on the activities in rat liver of some enzymes associated with glucose metabolism. Biochim. Biophys. Acta 411, 22–29.

Smith, J.L., Lear, S.R., Forte, T.M., Ko, W., Massimi, M., Erickson, S.K., 1998. Effect of pregnancy and lactation on lipoprotein and cholesterol metabolism in the rat. J. Lipid Res. 39, 2237–2249.

Spatling, L., Fallenstein, F., Huch, A., Huch, R., Rooth, G., 1992. The variability of cardiopulmonary adaptation to pregnancy at rest and during exercise. Br. J. Obstet. Gynaecol. 99, 1–40.

Symons, A.M., Turcan, R.G., Parke, D.V., 1982. Hepatic microsomal drug metabolism in the pregnant rat. Xenobiotica 12, 365–374.

Upreti, K., Chaki, S.P., Misro, M.M., 2002. Evaluation of peroxidative stress and enzymatic antioxidant activity during pregnancy and lactation in rats. Health Popul., Perspect. Issues 25, 177–185.

Williamson, D.H., 1986. Regulation of metabolism during lactation in the rat. Reprod. Nutr. Dev. 26, 597–603.

Available online at www.sciencedirect.com
SCIENCE DIRECT®
ELSEVIER
Experimental and Toxicologic Pathology 57 (2005) 15–28
EXPERIMENTAL AND TOXICOLOGIC PATHOLOGY
www.elsevier.de/etp

Microarray analysis of T-2 toxin-induced liver, placenta and fetal liver lesions in pregnant rats

Shinya Sehata[a,*], Naoki Kiyosawa[a], Fusako Atsumi[a], Kazumi Ito[a], Takashi Yamoto[a], Munehiro Teranishi[a], Koji Uetsuka[b], Hiroyuki Nakayama[b], Kunio Doi[b]

[a]*Medicinal Safety Research Laboratories, Sankyo Co., Ltd., 717 Horikoshi, Fukuroi-shi, Shizuoka 437-0065, Japan*
[b]*Department of Veterinary Pathology, Graduate School of Agricultural and Life Sciences, The University of Tokyo, 1-1-1 Yayoi, Bunkyo-ku, Tokyo 113-8657, Japan*

Received 4 November 2004; accepted 24 February 2005

Abstract

Pregnant rats on day 13 of gestation were treated orally with 2 mg/kg of T-2 toxin and sacrificed at 1, 3, 6, 9 and 12 h after the treatment (HAT). Histopathologically, the number of apoptotic cells was increased in the liver, placenta and fetal liver (peaked at 6, 12 and 9–12 HAT, respectively). To examine the gene expression profiles, we performed microarray analysis of these tissues at two selected time points based on the results of the TdT-mediated dUTP nick end labeling (TUNEL) staining. Increased expression of oxidative stress- and apoptosis-related genes was detected in the liver of dams, placenta and fetal liver of pregnant rats treated with T-2 toxin at the peak time point of apoptosis. Decreased expression of lipid metabolism- and drug-metabolizing enzyme-related genes was also detected in these tissues. The results suggested that the mitogen-activated protein kinase (MAPK) pathway might be involved in the mechanism of T-2 toxin-induced apoptosis. In addition, increased expression of the *c-jun* gene was consistently observed in these tissues. Our results suggest that the mechanism of T-2 toxin-induced toxicity in pregnant rats is due to oxidative stress followed by the activation of the MAPK pathway, finally inducing apoptosis. The *c-jun* gene may play an important role in T-2 toxin-induced apoptosis.

Keywords: T-2 toxin; Pregnant rats; Liver; Placenta; Fetal liver; Apoptosis; MAPK; Microarray

Introduction

T-2 toxin is a trichothecene mycotoxin produced by various species of *Fusarium* spp. *Fusarium* spp. occurs in cereals including corn, oats, rice and wheat. T-2 toxin has been found to contaminate foods, animal foods and agricultural products, and has been reported in many parts of the world (World Health Organization (WHO), 1990). A single dose or subacute dose of T-2 toxin induces damage in the lymphoid and hematopoietic tissues, resulting in lymphopenia and immunosuppression in

Abbreviations: ERK3, extracellular signal-related kinase 3; GD, gestation day; HAT, hours after treatment; HSP, heat shock protein; MAPK, mitogen-activated protein kinase; MEKK1, mitogen-activated protein kinase kinase 1; RT-PCR, reverse transcriptase-polymerase chain reaction; TUNEL, TdT-mediated dUTP nick end labeling

*Corresponding author. Tel.: +81 538 42 4356, fax: +81 538 42 4350.
E-mail address: sehata@sankyo.co.jp (S. Sehata).

0940-2993/$ - see front matter © 2005 Elsevier GmbH. All rights reserved.
doi:10.1016/j.etp.2005.02.005

many species (Marasas et al., 1969; Hoerr et al., 1981; Hayes and Schiefer, 1982; Pang et al., 1987; Shinozuka et al., 1998). These changes have been shown as being due to apoptosis (Sugamata et al., 1998). Furthermore, T-2 toxin has been shown to affect the central nervous system, although there have been no histopathological changes reported in the adult brain (Martin et al., 1986; WHO, 1990; Wang et al., 1998). It is also reported that pregnant mice treated with T-2 toxin exhibited fetal death and fetotoxicity mainly in the central nervous and skeletal systems in addition to maternal toxicity (Stanford et al., 1975; Rousseaux and Schiefer, 1987; Ishigami et al., 1999, 2001). We showed that apoptosis was observed in the thymus, liver, intestines, placenta, fetal brain and fetal liver at 24 and 48 h after treatment with T-2 toxin in pregnant rats on day 13 of gestation (Sehata et al., 2003). In rats, it is reported that T-2 toxin passes through the placenta and distributes to fetal tissues (Laferge-Frayssinet et al., 1990). Therefore, the apoptotic changes observed in the fetal tissues might be a direct effect of T-2 toxin. Although it is known that T-2 toxin induces lipid peroxidation, protein synthesis inhibition by interaction with ribosomes, and DNA synthesis inhibition (Chang and Mar, 1998; Middlebrook and Leatherman, 1989; Thompson and Wannemacher, 1990), the mechanism of T-2 toxin-induced toxicity is still unknown.

In recent years DNA microarray technologies have been developed. The application of this technology to the field of toxicology has been demonstrated including mycotoxin-induced toxicity. For example, Lühe et al. (2003) reported that ochratoxin A-specific transcriptional changes were detected for genes involved in DNA damage response and apoptosis, response to oxidative stress and inflammatory reactions. We performed microarray analysis of the liver, placenta and fetal liver from pregnant rats 24 h after T-2 toxin treatment (Sehata et al., 2004). According to the results, similar changes in the expression of apoptosis-, lipid metabolism-, drug metabolizing enzyme- and oxidative stress-related genes were detected in these tissues, suggesting that oxidative stress might be involved in the T-2 toxin-induced toxicity. In the above study, we only investigated the changes at 24 or 48 h after the T-2 toxin treatment. However, in general, it is considered that gene expression changes are early event in response to the exposure of chemicals. Therefore, to clarify the detailed mechanism of T-2 toxin-induced changes, earlier time point studies within 24 h after the treatment are necessary.

The purpose of the present study was to examine the detailed morphological changes and gene expression changes within 12 h after T-2 toxin treatment in the liver, placenta and fetal liver obtained from pregnant rats. The protocol of this study was approved by the Animal Care and Use Committee of the Graduate School of Agricultural and Life Sciences, The University of Tokyo.

Materials and methods

Animals

Forty-eight pregnant Wistar:Slc rats on day 11 of gestation (GD11) were obtained from Japan SLC Co., Ltd. (Hamamatsu, Japan). The animals were kept using an isolator caging system (Niki Shoji Co., Ltd., Tokyo, Japan) under controlled conditions (23±2 °C, 55±5% humidity and a 14-h light/10-h dark cycle), and fed commercial pellets (MF; Oriental Yeast Co., Ltd., Tokyo, Japan) and water ad libitum.

Treatments

Based on the results from the dose-finding study (data not shown) and a previously reported study of ours (Sehata et al., 2003), the animals were used on day 13 of gestation (GD13). GD13 is the middle day of organogenesis period in rats, and this period is thought to be sensitive to the chemical-induced toxicity. Therefore, we selected the animals on GD13 for the present study. T-2 toxin (Sigma Chemical Co., MO, USA) was dissolved in corn oil and a dosing volume was adjusted to 2.5 mL/kg. Eighteen animals were treated with a single oral dose of 2 mg/kg T-2 toxin (Sigma Chemical Co., St. Louis, MO, USA), and 3 animals were sacrificed for histopathological examination by exsanguination under ether anesthesia at 1, 3, 6, 9 and 12 h after treatment (HAT), respectively. For microarray analysis, based on the results of the histopathological examination, 9 rats were treated with T-2 toxin in the same way, and 3 rats were sacrificed at 3, 6 and 12 HAT, respectively. T-2 toxin was dissolved in corn oil and the dosing volume was adjusted to 2.5 ml/kg. In addition, a total of 24 animals that were treated with the vehicle alone were used as controls, and 3 animals were sacrificed at 1, 3, 6, 9 and 12 HAT, respectively.

Histopathological examination and immunohistochemical staining

After the animals were sacrificed, a macroscopic examination was performed. Dam's liver, placenta and fetuses from each dam were fixed in 10% neutral-buffered formalin to confirm the changes induced by T-2 toxin. Paraffin sections of 4 μm were stained with hematoxylin and eosin (HE) and subjected to microscopic examination. Cells with fragmented DNA were detected by the TdT-mediated dUTP nick end labeling (TUNEL) method using an apoptosis detection kit

(Apop Tag, Intergen, Purchase, NY, USA). In brief, multiple fragmented DNA-3′-OH ends on the section were labeled with digoxigenin-dUTP in the presence of terminal deoxynucleotidyl transferase (TdT). Peroxidase-conjugated anti-digoxigenin antibody was then reacted with the sections. Apoptotic nuclei were visualized by reacting with peroxidase-diaminobenzidine (DAB). The sections were then counterstained with methyl green. Morphometrical examination was performed in the liver, placenta and fetal telencephalon (3 fetuses/dam) in three randomly selected areas on the section under a light microscope (× 400). The number of positive cells/1000 cells was counted and the mean ± SE of the three measurements was calculated. Statistical analysis was carried out by the Student's *t*-test or Welch's *t*-test after analysis of homogeneity of variance by the *F*-test.

RNA extraction and microarray analysis

Based on the results of the histopathological examination, 9 rats were treated with T-2 toxin, and 3 rats were sacrificed at 3, 6 and 12 HAT, respectively. In addition, 9 rats were treated vehicle, and 3 rats were sacrificed at 3, 6 and 12 HAT, respectively. After the animals were sacrificed, the liver, placenta and fetuses were collected. The fetal liver was collected under stereoscopic microscope. The collected tissues were placed in the tubes and frozen in liquid nitrogen as soon as possible. The frozen tissues were kept under −80 °C until the analysis was performed. Total RNA was extracted from frozen tissues (up to 0.5 g) using the RNeasy Mini Kit (QIAGEN Inc., CA, USA) for the fetal liver or TRIzol reagent (Invitrogen, CA, USA) for the liver and placenta. The RNA from placenta and fetal liver from each dam were pooled to generate a single sample, respectively. The quality of the RNA samples was checked by spectrophotometry according to the Affymetrix protocol. Microarray analysis (total 36 arrays) was performed according to the Affymetrix protocol at the sampling time points (3, 6 and 12 HAT) based on the results of the morphometrical examination. Briefly, cDNA was prepared from 5 μg of total RNA using the SuperScript Choice System for cDNA Synthesis (Invitrogen, CA, USA), with the exception that the primer used for the reverse transcription reaction was a T7-$(dT)_{24}$ primer (primer sequence: 5′-GGC CAG TGA ATT GTA ATA CGA CTC ACT ATA GGG AGG CGG-$(dT)_{24}$-3′, Amersham Biosciences, Tokyo, Japan). Following this, biotin-labeled cRNA was synthesized from the cDNA using the Enzo High Yield RNA Transcription Labeling Kit (Enzo Diagnostics, NY, USA). After 20 μg of biotin-labeled cRNA was fragmented, a hybridization solution was prepared using a GeneChip® Eukaryotic Hybridization Control Kit (Affymetrix Inc., CA, USA) and hybridized to the Affymetrix Rat Genome U34A oligonucleotide array (including 8798 gene probes) at 45 °C for 16 h in a GeneChip® Hybridization Oven 640 (Affymetrix). The chips were washed and stained using the Fluidics Station (Affymetrix) and scanned with a GeneArray® Scanner (Affymetrix). Six chips (each 3 chips for control and T-2, respectively) were used for each time points. We performed the analysis at 3 and 6 HAT in the dam's liver, at 3 and 12 HAT in the placenta and the fetal liver. Therefore, total 36 chips were used.

Data analysis

The quality of the RNA samples used in the microarray analysis was checked by a 5′/3′ ratio of *GAPDH* housekeeping gene probes. The microarray imaging data were analyzed using Microarray Suite Version 5.0 (Affymetrix) and the Spotfire Pro Version 4.2 program (Spotfire Inc., MA, USA). In brief, total array normalization (global normalization after trimming the top 2% and bottom 2% of the data) was performed for all experimental data (Yang et al., 2001). Probes containing at least one *Absence Call* in the data were also removed. We selected genes that gave a mean value changes of greater than + 1.5 or less than −1.5. In addition, the mean value of each gene in the treated group was compared with that of the control group by the Student's *t*-test or the Welch's *t*-test after analysis of the homogeneity of variance by the *F*-test. A significance level of $p < 0.05$ was considered acceptable.

Real-time reverse transcriptase-polymerase chain reaction (RT-PCR)

GeneChip® results were confirmed by real-time RT-PCR for selected (Table 1). Total RNA (5 μg) from each sample was prepared as the same way described in *RNA extraction and microarray analysis*. RNA was treated with 5 U of DNase I (Takara, Shiga, Japan) in the manufacturer's buffer containing 40 U RNase inhibitor (TOYOBO, Osaka, Japan) in a final volume of 50 μL, and subjected to phenol-chloroform purification. DNase I-treated total RNA of 2 μg was reverse transcribed in a final volume of 20 μL using 200 U of SuperScript II (Invitrogen, CA, USA) in the manufacturer's buffer containing 10 mM DTT, 0.5 mM dNTPs, and 40 U of RNase inhibitor. Real-time PCR was performed using qPCR™ MasterMix Plus (Eurogentec, PA, USA), and the transcription was quantified with a GeneAmp® 5700 Sequence Detection System (Applied Biosystems, CA, USA). For internal control, Rodent GAPDH Control Kit (Applied Biosystems) was used. Statistical analysis for the mean values was carried out by the *F*-test followed by the Student's *t*-test or the Welch's *t*-test.

Table 1. Sequences of oligonucleotide primer/probe used for real-time RT-PCR

Gene (GenBank#)	Primer		TaqMan® probe
c-Jun	Forward	TGCAAAGATGGAAACGACCTT	ACGACGATGCCCTCAACGCCT
(X17163)	Reverse	CCACTCTCGGACTGGAGGAA	
MEKK1	Forward	TCCAGTAACATACACAGGGCAAAG	CATCCCGACCCGTTCCGG
(U48596)	Reverse	CATCCCCTAGTTTGCTTGTGCTA	
Bax-alpha	Forward	CCCCCCGAGAGGTCTTCTT	CGTGTGGCAGCTGACATGTTTGCA
(U59184)	Reverse	CGGCCCCAGTTGAAGTTG	
Heme oxygenase	Forward	TTCTTCTAGCGACAAGTTGATTCTGT	TCCTTGTACCATATCTATACGGCCCT
(J02722)	Reverse	GCTTGTTTCGCTCTATCTCCTCTT	
HSP70	Forward	TGGTGCAGTCGGACATGAA	CACTGGCCCTTCCAGGTGGTGAA
(Z27118)	Reverse	CGGGTAGAACGACCGGTTCT	

Results

Histopathological examination

The T-2 toxin treatment in pregnant rats induced histopathological change, apoptosis, in the liver of dams, placenta and fetal liver. Apoptosis of hepatocytes, cytotrophoblasts in the placenta, and hepatocytes and hematopoietic cells was confirmed by TUNEL staining (Fig. 1). The TUNEL-labeling index was increased at 1 HAT and peaked at 6 HAT in the liver of the dams by the treatment. The labeling index was increased at 1 HAT and was still increased at 12 HAT in the placenta. The labeling index was increased at 1 HAT, and reached a plateau after 9 HAT in the fetal liver (Fig. 2).

Microarray analysis

We selected the time points for microarray analysis based on the histopathological results. In particular, we selected the points at 3 HAT for the three tissues (before the peak time of apoptosis), at 6 HAT for the liver of dams (peak time point of apoptosis), and at 12 HAT for the placenta and fetal liver (peak time point of apoptosis). It is known that T-2 toxin induces apoptosis, lipid peroxidation and suppression of drug-metabolizing enzymes (Chang and Mar, 1998; Guerre et al., 2000; Sehata et al., 2004). Therefore, we focused on cell growth/apoptosis-, stress-, signal transduction-, and lipid- and other metabolism-related genes in the present study.

At 3 HAT in the liver of dams, the expression of 123 genes was increased and that of 140 genes was decreased by T-2 toxin treatment. The expression of the *heat shock protein* (*HSP*) *40-3* and *70* KDa *heat-shock-like protein* genes (stress-related genes) was increased. The expression of apoptosis-related genes such as the *RJG-9* gene for c-jun, *MEKK1* and *tumor necrosis factor receptor* was also increased. Increased expression of inflammation-related genes was detected. In addition, the expression of cell survival- or proliferation-related genes such as *RL/IF-1, p38 MAPK, ERK3* genes was also increased. On the other hand, the expression of lipid metabolism-related genes and drug-metabolizing enzyme genes (*CYP2A2, GST Yc2,* and *rGSTK1-1*) was suppressed by T-2 toxin (Table 2). At 6 HAT in the liver of dams, the peak time point of apoptosis, the expression of 218 genes was increased and that of 253 genes was decreased by T-2 toxin treatment. The expression of stress-related genes (*MnSOD, heme oxygenase* and *HSP86*) was increased. Apoptosis-related genes such as the *Bax-alpha, p21 protein (cip1), TGFB inducible early growth response, ICE-like cystein protease* and *protein kinase (MUK)* genes showed increased expression. In addition, the expression of cell survival- and proliferation-related genes (*NF-kappa B p105 subunit, Bcl2-like 13*) was also increased. On the other hand, the expression of lipid metabolism-related genes such as *17-beta hydroxysteroid dehydrogenase type 2* and *cholesterol 7-alpha-hydroxylas* genes, drug-metabolizing enzyme genes such as *P450d, P450e* and *GST Yc1* genes, and other metabolism-related genes was decreased. The expression of cell growth-related genes such as *cyclin D1* and *cyclin-dependent kinase 4* was also decreased (Table 3).

At 3 HAT in the placenta, the expression of 51 genes was increased and that of 21 genes was decreased by T-2 toxin treatment. The expression of stress-related genes such as the *oxidation resistance* and *NADPH-dependent thioredoxin reductase* genes was increased. The expression of apoptosis-related genes such as the *MEKK1* and *RL/IF-1* genes was increased (Table 4). At 12 HAT, the highest time point of apoptosis, the expression of 137 genes was increased and that of 123 genes was decreased by T-2 toxin treatment. The expression of stress-related genes such as the *HSP70*, and *metallothionein-2* and *-1* genes was increased. The expression of apoptosis-related genes (the *GADD45, p21 (c-Ki-ras),* and *RJG-9* gene for c-jun) was increased. The expression of the cell

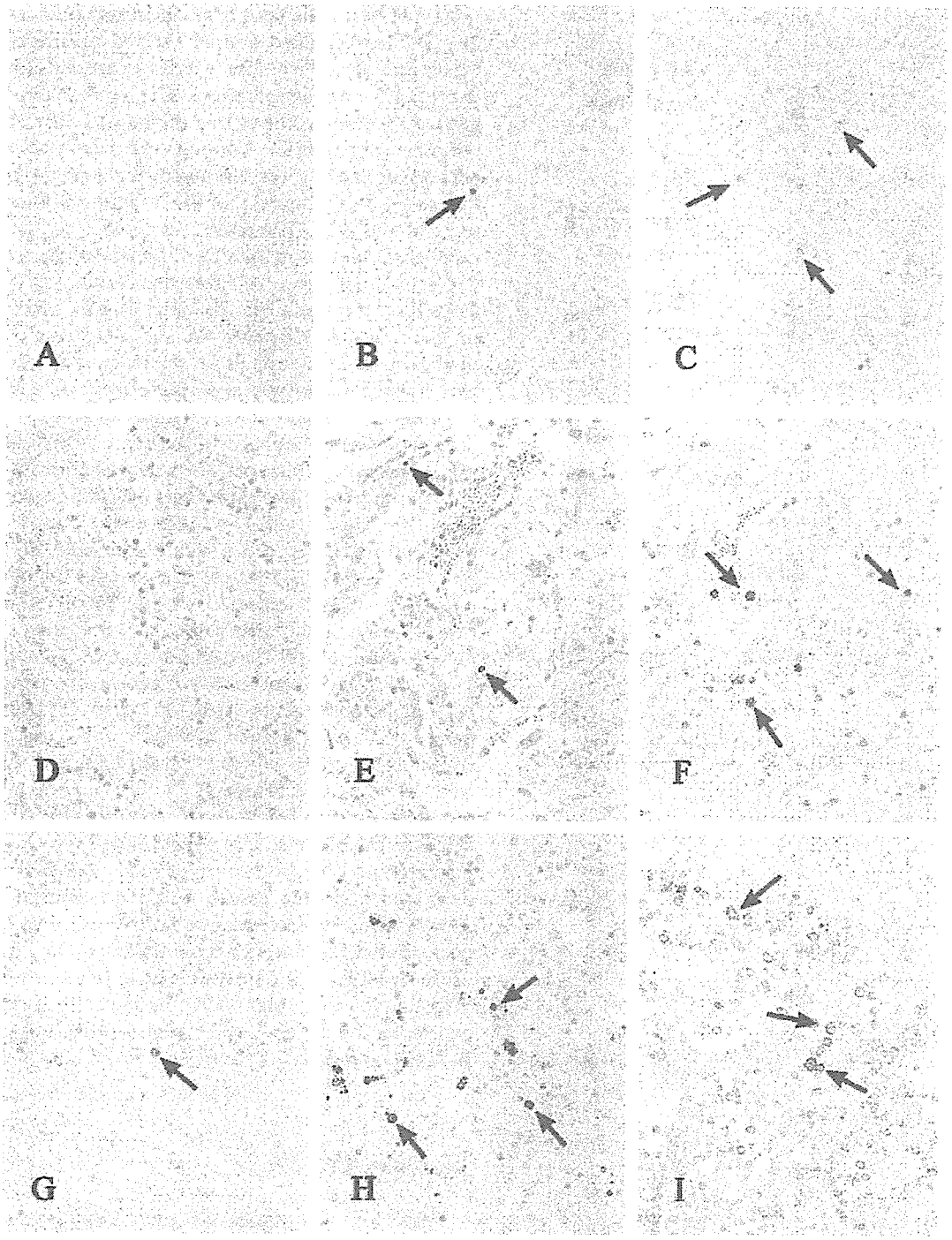

Fig. 1. TUNEL staining in the liver, placenta and fetal liver. The number of TUNEL-positive cells (arrow) was increased by T-2 toxin treatment. (A) A control liver at 12 HAT. (B) A T-2 toxin-treated liver at 3 HAT. (C) A T-2 toxin-treated liver at 12 HAT. (D) A control placenta at 12 HAT. (E) A T-2 toxin-treated placenta at 3 HAT. (F) A T-2 toxin-treated placenta at 12 HAT. (G) A control fetal liver at 3 HAT. (H) A T-2 toxin-treated fetal liver at 3 HAT. (I) A T-2 toxin-treated fetal liver at 12 HAT. TUNEL staining. × 100 (A–C), × 200 (D–I).

survival-related gene (*NF-kappa B p105 subunit*) was also increased. In addition, the expression of inflammation-related genes was also increased. On the other hand, the expression of the lipid metabolism-related genes such as *squalene epoxidase* and *7-dehydrocholesterol reductase* genes, and a drug-metabolizing enzyme

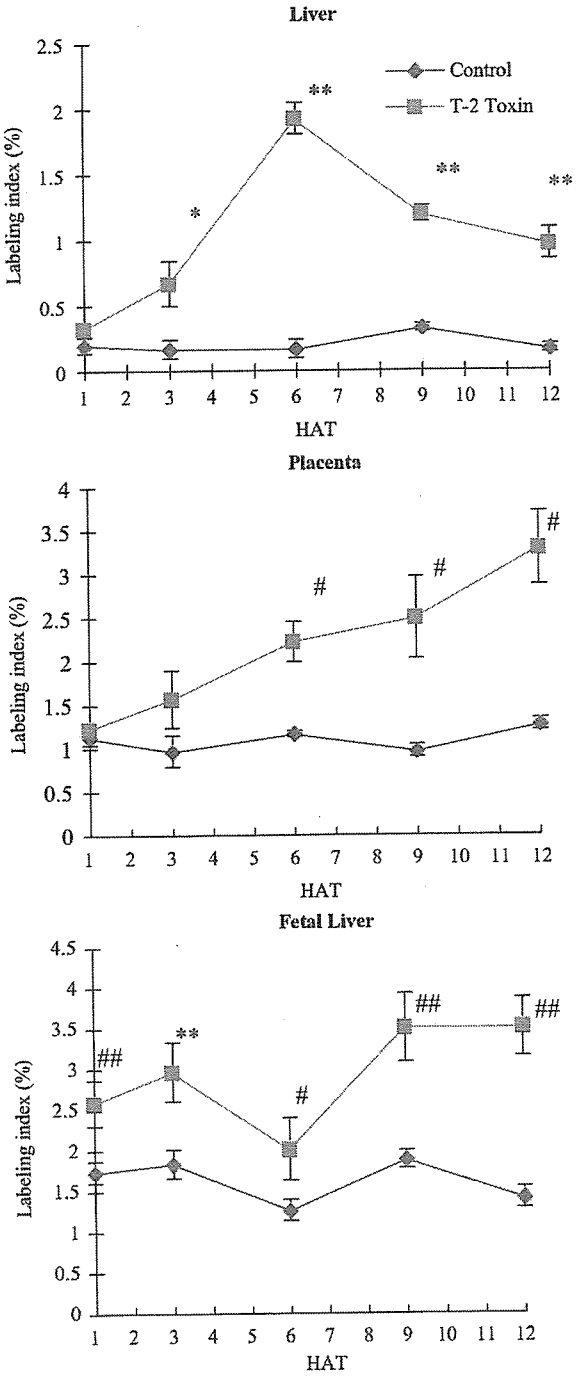

Fig. 2. TUNEL labeling indices in the liver, placenta and fetal liver. The peak time of TUNEL-positive cells was obtained at 6 HAT in the liver, at 12 HAT in the placenta. In the fetal liver, the number of TUNEL-positive cells increased from 1 HAT, and reached a plateau from 9 HAT. Mean±SE. Significantly difference from control: $^{*}p<0.05$, $^{**}p<0.01$ (Student's *t*-test); $^{\#}p<0.05$, $^{\#\#}p<0.01$ (Welch's *t*-test).

gene (*GST Yb*) was decreased. The expression of cell cycle-related genes (*cyclin D1, D3* and *cyclin-dependent kinase 4*) was also decreased (Table 5).

At 3 HAT of the fetal liver, the result obtained from one T-2 toxin-treated animal showed a different gene expression profile from the other two animals (data not shown). The number of fetuses of this animal was 7. The gene expression profile of this animal was different from the other two animals. Although the reason of different expression pattern was unknown, there might be some differences in the severity of the lesion in each obtained fetus of the dam. Therefore, we considered that small number of fetuses might be affected to the obtained data, and that this result was not enough to analysis. Therefore, we excluded the data of the animal from further analysis. However, we show the results of the other two treated-animals as reference data (Table 6). No statistical analysis was performed on this data because of the small number of animals. At 12 HAT, the peak time point of apoptosis, the expression of 86 genes was increased and that of 227 genes was decreased by T-2 toxin treatment. The expression of stress-related genes (*metallothionein-2* and *-1*) was increased. The expression of apoptosis-related genes such as the *Bax, Bax-alpha, Bcl-X-long, GADD45* genes, *RJG-9* genes for c-jun and *c-fos* gene was increased. On the other hand, the expression of lipid metabolism-related genes such as *mitochondrial HMG Co-A synthase* and *17-beta hydroxysteroid dehydrogenase type 2* genes, and drug-metabolizing enzyme genes (*GST Yc2* and *CYP4A3*) was decreased. The expression of cell survival- and apoptosis-related genes (*cyclin D1, p38 MAPK* and *Makp14*) was also decreased (Table 7).

The genes detected in the three tissues are shown in Table 8. The expression of the *RJG-9* gene for c-jun was increased and the expression of the *cyclin D1* gene was decreased in all the tissues. The expression of the *p38 MAPK* gene was increased in the liver of dams and was decreased in the placenta and fetal liver. The expression of the *NF-kappa B* gene and related *RL/IF-1* gene was increased in the liver and placenta of dams. The expression of the *Bax-alpha* gene was increased in the liver of dams and fetal liver.

Real-time RT-PCR

Based on the results of microarray analysis and histopathological examinations (apoptosis), oxidative stress- and apoptosis-related genes were selected to confirm the changes observed in the microarray analysis. Real-time RT-PCR analysis was performed for selected genes and the time points that showed changes in the microarray analysis. The results showed increased expression of the *c-jun, MEKK1, Bax-alpha, HSP70* and *heme oxygenase* genes by T-2 toxin treatment (Fig. 3). Although not all results were completely consistent with those of the microarray analysis,

Table 2. Gene expression changes observed in the dam's liver at 3 HAT

Gene	Function	GenBank#	Fold change	*t*-test
Up-regulated				
Heat shock protein hsp40-3	Stress	AA891542	2.61	0.000
70 kd heat-shock-like protein	Stress	M11942	1.92	0.038
Thioredoxin-like (32kD)	Stress	AA891694	1.74	0.015
PRG1	Cell growth	X96437	3.49	0.045
RJG-9 gene for c-jun	Transcription	AI175959	120.21	0.021
RL/IF-1	Transcription	X63594	25.78	0.014
LIM protein FHL2 (Fhl2)	Transcription	AA891527	2.50	0.044
3CH134/CL100 PTPase (oxidative stress-inducible protein tyrosine phosphatase)	Signal transduction	S81478	11.50	0.018
MAP kinase kinase kinase 1 (MEKK1)	Signal transduction	U48596	2.59	0.001
p38 mitogen activated protein kinase	Signal transduction	AA924542	2.09	0.040
Extracellular signal-related kinase (ERK3)	Signal transduction	M64301	2.01	0.008
14-3-3 protein	Signal transduction	D30740	1.85	0.000
Soluble IL-1 receptor type I	Receptor	U14010	6.43	0.000
Interleukin-1 receptor type I	Receptor	M95578	5.18	0.018
Tumor necrosis factor receptor	Receptor	M63122	2.98	0.000
Macrophage inflammatory protein-1alpha	Inflammation	U22414	28.06	0.000
Down-regulated				
Glycerol 3-phosphate acyltransferase	Lipid metabolism	U36771	−6.62	0.008
Trihydroxycoprostanoyl-CoA Oxidase	Lipid metabolism	X95189	−2.43	0.002
Apolipoprotein A-I (apoA-I)	Lipid metabolism	M00001	−2.37	0.015
Hydroxysteroid dehydrogenase, 11 beta type 1 (Hsd11b1)	Lipid metabolism	AI105448	−2.02	0.002
Cytochrome P-450-LA-omega (lauric acid omega-hydroxylase)	Drug metabolizing enzyme	AA924267	−2.44	0.001
Cytochrome P450 IIA2 protein (CYP2A2)	Drug metabolizing enzyme	J04187	−1.55	0.005
GST Yc2	Drug metabolizing enzyme	AA945082	−1.69	0.030
rGSTK1-1 (glutahione S-transferase subunit 13)	Drug metabolizing enzyme	AI105137	−1.53	0.036
Insulin growth factor-binding protein	Cell growth	J04486	−1.89	0.006
CDK5 activator-binding protein C53	Cell growth	AA799745	−1.56	0.003
CyclinG-associated kinase	Cell growth	D38560	−1.55	0.033

individual data showed a good correlation with those of the microarray analysis.

Discussion

T-2 toxin induces apoptosis in the lymphoid tissues and intestine. T-2 toxin also has fetotoxicity. We previously reported the histopathological changes in pregnant rats, and the number of apoptotic cells was increased in the liver of dams, placenta and fetal liver at 24 and 48 h after the T-2 toxin treatment (Sehata et al., 2003). It is reported that apoptosis induction by T-2 toxin involved activation of caspase-3 and -9 (Nagase et al., 2001). Yang et al. (2000) reported that apoptosis induction by satratoxins and other trichothecenes might involve the MAPK pathway. However, these studies were in vitro studies and T-2 toxin-induced toxicity in pregnant animals was still unclear. We performed microarray analysis of the liver, placenta and fetal liver from pregnant rats at 24 h after the T-2 toxin treatment, and showed that apoptosis-, oxidative stress-, lipid metabolism- and other metabolism-related genes were detected in all these tissues, suggesting that these factors may be involved in the T-2 toxin-induced toxicity (Sehata et al., 2004). However, in general, it is considered that gene expression changes are early event in response to the exposure of chemicals. In the present study, we performed microarray analysis at an earlier time point of the liver, placenta and fetal liver from pregnant rats treated with T-2 toxin. We also performed real-time RT-PCR analysis in selected genes and we confirmed that both data showed a good correlation.

From the results of the microarray analysis, the expression of oxidative stress-related genes such as the *HSP40, heme oxygenase* and *MnSOD* genes in the liver, *thioredoxin reductase, HSP70* and *metallothionein-2* and

Table 3. Gene expression changes observed in the dam's liver at 6 HAT

Gene	Function	GenBank#	Fold change	*t*-test
Up-regulated				
Manganese-containing superoxide dismutase (MnSoD)	Stress	Y00497	10.00	0.009
Heme oxygenase	Stress	J02722	2.20	0.008
hsp86	Stress	AA819776	1.55	0.040
Similar to growth arrest and DNA-damage-inducible 45 alpha	Cell growth	AI070295	69.41	0.030
p21 protein (cip1)	Cell growth	L41275	18.44	0.041
Transformed mouse 3T3 cell double minute 2 (Mdm2)	Cell growth	AI639488	11.30	0.008
Nuclear factor kappa B p105 subunit	Cell growth	L26267	11.25	0.035
TGFB inducible early growth response (Tieg)	Cell growth	AI071299	8.22	0.020
Bcl2-like 13 (apoptosis facilitator)	Cell growth	AA892271	1.73	0.012
Bax-alpha	Cell growth	U59184	1.61	0.014
Cbp/p300-interacting transactivator with Glu/Asp-rich carboxy-terminal domain 2 (Cited2)	Transcription	AA900476	8.91	0.042
Heat shock transcription factor 1	Transcription	AI172097	3.18	0.005
Protein-tyrosine kinase (JAK2)	Signal transduction	U13396	6.62	0.004
Smad1 protein (Smad1)	Signal transduction	AF067727	3.65	0.004
ICE-like cysteine protease (Lice)	Signal transduction	U49930	3.27	0.025
Protein kinase (MUK)	Signal transduction	D49785	2.29	0.010
TANK-binding kinase 1	Signal transduction	AI639447	2.26	0.024
p38 mitogen activated protein kinase (Mapk14)	Signal transduction	AI171630	1.80	0.010
Alpha-2-macroglobulin	Inflammation	M22670	49.75	0.003
Tumor necrosis factor receptor superfamily 1b	Receptor	AA900380	4.97	0.012
CC chemokine receptor protein	Receptor	E13732	2.52	0.018
Down-regulated				
17-Beta hydroxysteroid dehydrogenase type 2	Lipid metabolism	X91234	−4.48	0.024
Cholesterol 7-alpha-hydroxylase	Lipid metabolism	J05460	−4.29	0.025
Acyl coenzyme A dehydrogenase medium chain	Lipid metabolism	J02791	−3.33	0.004
Carnitine octanoyltransferase	Lipid metabolism	U26033	−2.70	0.004
Apolipoprotein A-IV	Lipid metabolism	M00002	−2.19	0.001
Cytochrome P-450d	Drug metabolism	K03241	−4.57	0.003
Cytochrome P-450e	Drug metabolism	M13234	−3.76	0.001
Cytochrome P-450b (phenobarbital-inducible)	Drug metabolism	L00320	−2.75	0.029
Cytochrome P-450 IV A1 (CYP4A1)	Drug metabolism	M57718	−2.59	0.021
Liver UDP-glucuronosyltransferase, phenobarbital-inducible form	Drug metabolism	M13506	−2.62	0.019
Glutathione S-transferase Yc2 subunit	Drug metabolism	S72506	−2.18	0.029
Max interacting protein 1 (Mxi1)	Cell growth	AA893611	−2.72	0.001
Cyclin-dependent kinase 4 (cdk4)	Cell growth	L11007	−2.12	0.012
DNase gamma	Cell growth	U75689	−2.10	0.015
Cyclin D1	Cell growth	D14014	−1.93	0.001
Cell cycle progression related D123	Cell growth	U34843	−1.77	0.031

Table 4. Gene expression changes observed in the placenta at 3 HAT

Gene	Function	GenBank#	Fold change	*t*-test
Up-regulated				
Oxidation resistance 1 (Oxr1)	Stress	H33461	1.68	0.047
NADPH-dependent thioredoxin reductase (TRR1)	Stress	AA891286	1.52	0.014
Cytocentrin	Cell growth	U82623	2.12	0.013
RL/IF-1	Transcription	X63594	1.55	0.035
Similar to mitogen-activated protein kinase kinase kinase 1 (MAPK/ERK kinase kinase 1) (MEK kinase 1) (MEKK 1)	Signal transduction	AI102620	1.56	0.012
Down-regulated				
Decorin	Signal transduction	AI639233	−2.02	0.030

Table 5. Gene expression changes observed in the placenta at 12 HAT

Gene	Function	GenBank#	Fold change	*t*-test
Up-regulated				
Heat shock protein 70	Stress	Z27118	7.74	0.047
Metallothionein-2 and metallothionein-1	Stress	AI176456	1.64	0.000
Macrophage inflammatory protein-2 precursor	Inflammation	U45965	14.53	0.007
Interleukin 1-beta	Inflammation	M98820	2.92	0.006
Nerve growth factor induced factor A	Cell growth	AF023087	13.27	0.026
Mdm2	Cell growth	AI639488	2.86	0.031
GADD45	Cell growth	L32591	2.21	0.045
P21 (c-Ki-ras)	Cell growth	U09793	1.56	0.019
v-Jun sarcoma virus 17 oncogene homolog (avian) (Jun)	Transcription	AA945867	2.94	0.017
RJG-9 gene for c-jun	Transcription	AI175959	2.83	0.004
RL/IF-1	Transcription	X63594	2.25	0.005
Nuclear factor kappa B p105 subunit	Transcription	L26267	2.20	0.000
c-Jun oncogene mRNA for transcription factor AP-1	Transcription	X17163	2.08	0.022
Cbp/p300-interacting transactivator with Glu/Asp-rich carboxy-terminal domain 2 (Cited2)	Transcription	AA900476	1.80	0.003
Protein-tyrosine phosphatase	Signal transduction	X58828	2.06	0.008
3CH134/CL100 PTPase (oxidative stress-inducible protein tyrosine phosphatase)	Signal transduction	S81478	1.69	0.035
Down-regulated				
Squalene epoxidase	Lipid metabolism	D37920	−2.60	0.008
7-Dehydrocholesterol reductase	Lipid metabolism	AB016800	−2.34	0.016
Glutathione S-transferase (GST) Y(b) subunit	Drug metabolizing enzyme	X04229	−1.97	0.003
Insulin-like growth factor-binding protein (IGF-BP3)	Cell growth	M31837	−2.16	0.003
Cyclin-dependent kinase 4 (cdk4)	Cell growth	L11007	−2.07	0.013
Cyclin D3	Cell growth	D16309	−1.98	0.004
Cyclin D1	Cell growth	D14014	−1.52	0.007
MASH-2	Transcription	X53724	−2.28	0.013
p38 Mitogen activated protein kinase	Signal transduction	U73142	−1.96	0.015
Similar to mitogen activated protein kinase kinase kinase kinase 1	Signal transduction	AA891302	−1.52	0.040
LDL-receptor	Receptor	X13722	−2.27	0.010
Pregnancy-specific beta 1-glycoprotein	Cell adhesion	U66292	−3.63	0.009
Spongiotrophoblast specific protein	Cell adhesion	AB009890	−3.11	0.025
Carcinoembryonic antigen-related protein	Cell adhesion	L00686	−2.78	0.004

Table 6. Gene expression changes observed in the fetal liver at 3 HAT (reference data)

Genes	Function	GenBank#	Fold change
Up-regulated			
CC chemokine ST38 precursor	Inflammation	AF053312	2.20
Mob-1	Inflammation	U17035	1.58
Interferon-gamma inducing factor isoform alpha precursor (IGIF)	Inflammation	U77777	1.52
Krox20	Transcription	U78102	1.60
Pregnancy-specific glycoprotein (rnCGM3)	Cell adhesion	U09815	1.89
Vascular cell adhesion molecule-1	Cell adhesion	M84488	1.54
Down-regulated			
Oxidosqualene lanosterol-cyclase	Lipid metabolism	E12275	−2.08
Acyl-CoA hydrolase	Lipid metabolism	AB010428	−2.00
Cytochrome P450 arachidonic acid epoxygenase (cyp 2C23)	Drug metabolism	U04733	−1.56
Glutathione s-transferase M5	Drug metabolism	U86635	−1.61
Growth arrest and DNA-damage-inducible protein GADD153	Cell growth	U30186	−3.13
Glioma-derived vascular endothelial cell growth factor	Cell growth	M32167	−1.52
Insulin-like growth factor I	Cell growth	M81183	−1.52
Caspase 6 (Mch2)	Signal transduction	AF025670	−1.54

Table 7. Gene expression changes observed in the fetal liver at 12 HAT

Gene	Function	GenBank#	Fold change	t-test
Up-regulated				
Metallothionein-2 and metallothionein-1	Stress	AI176456	9.37	0.000
Adrenomedullin precursor	Cell growth	D15069	4.37	0.039
Vascular endothelial growth factor A (VEGFA)	Cell growth	AA850734	2.88	0.003
MGADD45	Cell growth	L32591	2.30	0.009
Bax	Cell growth	S76511	1.73	0.034
Bax-alpha	Cell growth	U59184	1.51	0.031
Programmed cell death repressor BCL-X-Long	Cell growth	U34963	1.69	0.034
Mud-4	Cell growth	U70270	1.64	0.019
Gas-5 growth arrest homolog non-translated mRNA sequence	Cell growth	U77829	1.55	0.023
RJG-9 gene for c-jun	Transcription	AI175959	3.12	0.002
Cbp/p300-interacting transactivator with	Transcription	AA900476	2.19	0.004
Glu/Asp-rich carboxy-terminal domain 2 (Cited2) c-Fos	Transcription	X06769	2.02	0.019
Down-regulated				
Mitochondrial 3-hydroxy-3-methylglutaryl-CoA synthase	Lipid metabolism	M33648	−6.95	0.002
3-Hydroxy-3-methylglutaryl-Coenzyme A synthase 1 (Hmgcsl)	Lipid metabolism	AI177004	−3.13	0.024
17-Beta hydroxysteroid dehydrogenase type 2	Lipid metabolism	X91234	−4.02	0.025
Farnesyl diphosphate synthase (Fdps)	Lipid metabolism	AI180442	−3.64	0.014
Glutathione S-transferase Yc2 subunit	Drug metabolizing enzyme	S72506	−4.39	0.026
GST Yc2	Drug metabolizing enzyme	AA945082	−3.52	0.005
Cytochrome P-450-LA-omega (lauric acid omega-hydroxylase)	Drug metabolizing enzyme	AA997806	−3.04	0.026
Cyp4a locus encoding cytochrome P450 (IVA3)	Drug metabolizing enzyme	M33936	−2.98	0.023
Cytochrome P-450	Drug metabolizing enzyme	D13912	−2.55	0.006
Cyclin Dl	Cell growth	D14014	−2.12	0.005
Cyclin E	Cell growth	D14015	−1.52	0.011
p38 Mitogen activated protein kinase	Signal transduction	U73142	−2.46	0.002
p38 Mitogen activated protein kinase (Mapkl4)	Signal transduction	AI171630	−1.79	0.006
ICE-like cysteine protease (Lice)	Signal transduction	U49930	−2.04	0.017
MEK5alpha-l (MEK5)	Signal transduction	U37462	−1.75	0.018
14-3-3 Protein theta-subtype	Signal transduction	D17614	−1.70	0.024
Programmed cell death 8 (apoptosis-inducing factor)	Signal transduction	AA891591	−1.53	0.014

-1 in the placenta, and *metallothionein-2* and *-1* in the fetal liver increased. The real-time RT-PCR also confirmed the increased expression of *HSP70* in the placenta and the increased expression of *heme oxygenase* in the liver of dams. It is known that oxidative stress evokes various cellular events including apoptosis, growth arrest and activation of transcription factors. Oxidative stress causes lipid peroxidation and induces mitochondrial dysfunction. Mitocondrial dysfunction causes fatty acid β-oxidation and induces fatty liver (Jaeschke et al., 2002). T-2 toxin enhances lipid peroxidation (Chang and Mar, 1998). In addition, fatty liver was observed in the liver in our previous study (Sehata et al., 2003). The microarray results in the present study showed that the decreased expression of lipid metabolism-related genes suggested that the disturbance of lipid metabolism caused by oxidative stress occurred in the dam's liver, placenta and fetal liver by T-2 toxin.

Increased apoptosis in the liver of dams, placenta and fetal liver was observed histopathologically in this study. The expression of apoptosis-related genes such as the *GADD45, p21, cyclin D1, NF-kappa B, Bax-alpha, mdm2, c-jun, MEKK1, p38 MAPK* and *ERK3* genes, was changed by T-2 toxin treatment. MAPKs are important intermediates in signaling pathways for responding to extracellular stress. MAPKs play a role in cell growth, differentiation and apoptosis. For example, ERK mediates cell growth and protects cells from apoptosis, whereas JNK (c-Jun N-terminal kinase)

Table 8. Gene expression changes observed in the dam's liver, placenta and fetal liver

Gene	Function	GenBank#	Fold change				
			Liver		Placenta		Fetla liver
			3 HAT	6 HAT	3 HAT	12 HAT	12 HAT
All tissues							
Oxidation resistance 1 (Oxr1)	Stress	H33461		−1.87	1.68		−1.90
Protein disulfide isomerase-related protein (P5-pending)	Stress	AA892532		−1.81		−1.61	−1.59
Progression elevated gene 3 protein	Cell growth	AF020618	16.77			2.26	2.58
PRG1	Cell growth	X96437	3.49			2.13	1.70
Cyclin D1	Cell growth	D14014		−1.93		−1.52	−2.12
RJG-9 gene for c-jun	Transcription	AI175959	120.21			2.83	3.12
Cbp/p300-interacting transactivator with Glu/Asp-rich carboxy-terminal domain 2 (Cited2)	Transcription	AA900476		8.91		1.80	2.19
TIS 11	Immediate early gene	X63369	21.37			1.59	1.67
Initiation factor eIF-2B gamma subunit (eIF-2B gamma)	Translation	U38253		2.03		1.84	1.54
Protein tyrosine phosphatase	Signal transduction	U02553	8.45			1.97	3.45
p38 Mitogen activated protein kinase	Signal transduction	U73142	1.87			−1.96	−2.46
Glycoprotein processing glucosidase I	Metabolism	AF087431		−1.52		−1.73	−2.13
H2A and H2B histones	Cell structure	X59961		1.85		1.93	1.57
Liver and Placenta							
Transformed mouse 3T3 cell double minute 2 (Mdm2)	Cell growth	AI639488		11.30		2.86	
Nuclear factor kappa B p105 subunit	Cell growth	L26267		11.25		2.20	
Cyclin-dependent kinase 4 (cdk4)	Cell growth	L11007		−2.12		−2.07	
RL/IF-1	Transcription	X63594	25.78		1.55	2.25	
3CH134/CL100 PTPase	Signal transduction	S81478	11.50			1.69	
Glutathione S-transferase (GST) Y(b) subunit	Drug metabolism	X04229	1.55			−1.97	
Liver and Fetal liver							
Bax-alpha	Cell growth	U59184		1.61			1.51
p38 Mitogen activated protein kinase	Signal transduction	AA924542	2.09				−1.52
ICE-like cysteine protease (Lice)	Signal transduction	U49930		3.27			−2.04
17-Beta hydroxysteroid dehydrogenase type 2	Lipid metabolism	X91234		−4.48			−4.02
Cytochrome P-450	Drug metabolism	D13912		−2.34			−2.55
Glutathione S-transferase Yc2 subunit	Drug metabolism	S72506		−2.18			−4.39
Placenta and Fetal liver							
Metallothionein-2 and metallothionein-1	Stress	AI176456				1.64	9.37
GADD45	Cell growth	L32591				2.21	2.30
7-Dehydrocholesterol reductase	Lipid metabolism	AB016800				−2.34	−2.28

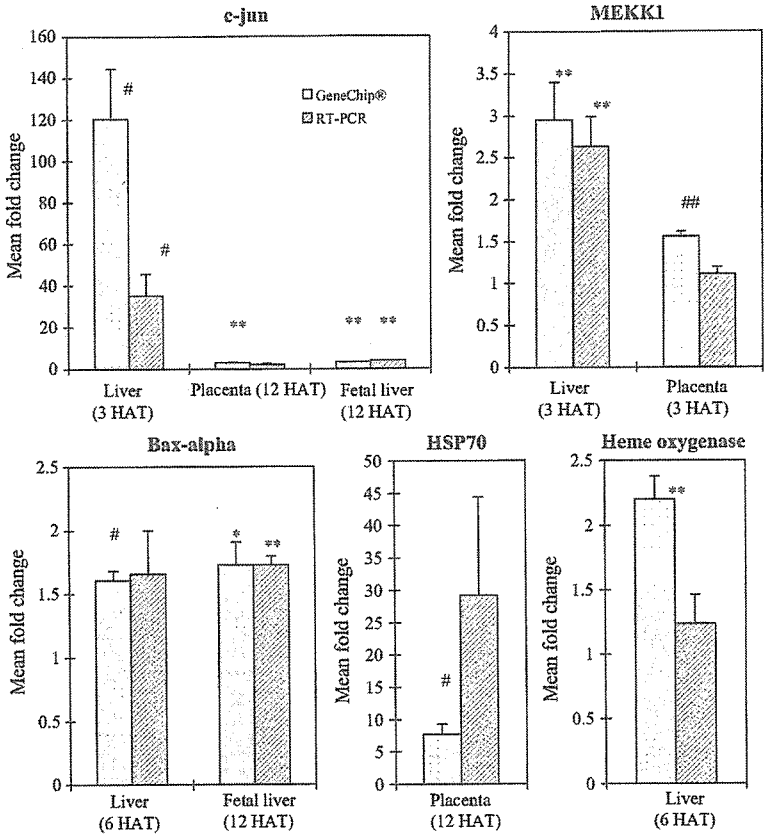

Fig. 3. Comparison of the fold changes in T-2 toxin-treated animals obtained from GeneChip® analysis and real-time RT-PCR analysis. The results of real-time RT-PCR (▨) showed a good correlation to that of GeneChip® analysis (□). Mean±SE. Significantly different from control: $^{*}p<0.05$, $^{**}p<0.01$ (Student's *t*-test); $^{\#}p<0.05$, $^{\#\#}p<0.01$ (Welch's *t*-test).

and p38 MAPK inhibit cell proliferation and may promote apoptosis (Jarpe et al., 1998). Each MAPK is activated by an upstream MAPK kinase, including MEKK1, and activates transcription factors such as c-jun and c-fos. MEKK1 may induce apoptosis by causing a general deregulation of MAPK signaling (Boldt et al., 2003). In the present study, MAPK genes were detected by T-2 toxin treatment as described above. The real-time RT-PCR confirmed the increased expression of *MEKK1* gene. Increased expression of the *c-jun* gene was detected in all three tissues both in the microarray analysis and real-time RT-PCR analysis. c-Jun may also play a role in induction of apoptosis (Leppä and Bohmann, 1999). For example, negative regulation of NF-kappa B-dependent transcription of c-jun contributes to cisplatin-induced cell death (Sánchez-Pérez et al., 2002). NF-kappa B is generally involved in suppression of apoptosis by activating the expression of antiapoptotic genes (Kucharczak et al., 2003). However, NF-kappa B also plays a vital role in p53-mediated apoptosis (Ryan et al., 2000). Furthermore, NF-kappa B is a mediator of stress-induced gene expression. It is also known that MAPKs are involved in the NF-kappa B activation pathway (Mercurio and Manning, 1999). Therefore, the MAPK pathway may be involved in the mechanism of T-2 toxin-induced toxicity, and among many factors involved in this pathway, c-jun may play an important role in apoptosis induction (Fig. 4). In addition, increased expression of the *Bax-alpha* gene was detected in both liver and fetal liver. The real-time RT-PCR also confirmed the increased expression of the *Bax-alpha* gene in the liver and fetal liver. Bax is a member of the bcl-2 family and induces apoptosis. It is also reported that apoptosis induction in HL60 cells by T-2 toxin involved activation of caspase-3 and -9 through the release of cytochrome c from mitochondria in the cytosol (Nagase et al., 2001). Therefore, at least in the hepatic tissues, the Bax and caspase pathways may be involved in the mechanism of T-2 toxin-induced toxicity. On the other hand, increased expression of the *GADD45* and *p21* genes, and decreased expression of the *cyclin D1* gene were observed. This suggested that growth arrest or cell repair also occurred at the same time.

It is reported that the expression of phase I and II enzyme genes was decreased by T-2 toxin (Galtier et al., 1989; Guerre et al., 2000). We reported that decreased

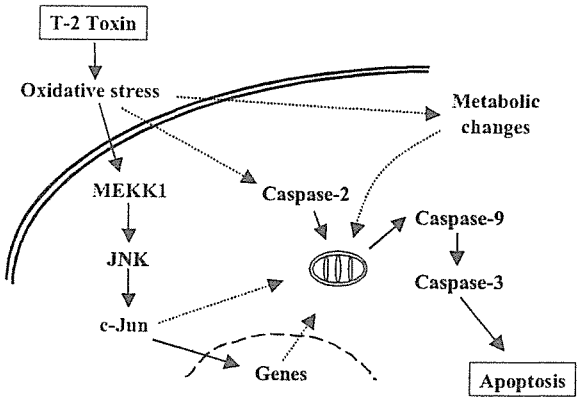

Fig. 4. Speculated mechanisms of T-2 toxin-induced toxicity in pregnant rats.

expression of drug-metabolizing enzyme genes was observed in the liver, placenta and fetal liver of pregnant rats at 24 HAT (Sehata et al., 2004). In the present study, decreased expression of drug-metabolizing enzyme genes was also observed in these tissues, indicating that this suppressive effect by T-2 toxin was a relatively early event.

When compared the differences in gene expression profiles in these tissues, the number of metabolism-related genes in the placenta was smaller than those in the dam's liver and fetal liver. This suggests that the placenta might play a less role in T-2 toxin metabolism. It is known that the expression of P450 genes in the fetal liver is different in the gestational days. The differences in the expression of P450 genes in the dam's liver and fetal liver obtained in the present study might reflect the difference of the basic expression of P450 genes in these tissues. In the placenta, we detected the decreased expression of cell adhesion-related genes, pregnancy-specific beta 1-glycoprotein, spongiotrophoblast specific protein and carcinoembryonic antigen-related protein. These genes express specifically in the placenta. As we do not know whether this change may reflect the morphological changes (apoptosis in cytotrophoblasts) or not, and specific in the placenta, we should examine the relation of T-2 toxin-induced apoptosis and cell adhesion changes in the other tissues more detail.

In the present study, the expression of oxidative stress-, apoptosis-, lipid metabolism- and drug-metabolizing enzyme-related genes was changed in the liver, placenta and fetal liver from pregnant rats treated with T-2 toxin. As regarding apoptosis, the MAPK pathway may be involved in the mechanism of T-2 toxin-induced apoptosis. In addition, increased expression of the *c-jun* gene was consistently observed in these tissues, suggesting that c-jun may be a key factor. In conclusion, it is speculated that in the mechanism of T-2 toxin-induced toxicity in pregnant rats, T-2 toxin induces oxidative stress, following by activation of the MAPK pathway, finally inducing apoptosis (Fig. 4). And the *c-jun* gene may play an important role in the induction of apoptosis. Further detailed studies are necessary to clarify the mechanism of T-2 toxin-induced toxicity.

Acknowledgements

We thank Mrs. K. Hara for preparation of histopathological samples, and Mrs. K. Watanabe and Mrs. N. Niino for conducting the microarray and real-time RT-PCR analyses.

References

Boldt S, Weidle UH, Kolch W. The kinase domain of MEKK1 induces apoptosis by dysregulation of MAP kinase pathways. Exp Cell Res 2003;283:80–90.

Chang IM, Mar WC. Effect of T-2 toxin on lipid peroxidation in rats: elevation of conjugated diene formation. Toxicol Lett 1998;40:275–80.

Galtier P, Paulin F, Eeckhoutte C, et al. Comparative effects of T-2 toxin and diacetoxyscirpenol on drug metabolizing enzymes in rat tissues. Food Chem Toxicol 1989;27:215–20.

Guerre P, Eeckhoutte C, Burgat V, et al. The effects of T-2 toxin exposure on liver drug metabolizing enzymes in rabbit. Food Addit Contam 2000;17:1019–26.

Hayes MA, Schiefer FB. Comparative toxicity of dietary T-2 toxin in rats and mice. J Appl Toxicol 1982;2:207–12.

Hoerr FJ, Carlton WW, Yagen B. Mycotoxicosis caused by a single dose of T-2 toxin or diacetoxyscirpenol in broiler chickens. Vet Pathol 1981;18:652–64.

Ishigami N, Shinozuka J, Katayama K, et al. Apoptosis in the developing mouse embryos from T-2 toxin-inoculated dams. Histol Histopathol 1999;14:729–33.

Ishigami N, Shinozuka J, Katayama K, et al. Apoptosis in mouse fetuses from dams exposed to T-2 toxin at different days of gestation. Exp Toxicol Pathol 2001;52:493–501.

Jaeschke H, Gores GJ, Cederbaum AI, et al. Mechanisms of hepatotoxicity. Toxicol Sci 2002;65:166–76.

Jarpe MB, Widmann C, Knall C, et al. Anti-apoptotic versus pro-apoptotic signal transduction: checkpoints and stop signs along the road to death. Oncogene 1998;17:1475–82.

Kucharczak J, Simmons MJ, Fan Y, et al. To be, or not to be: NF-κB is the answer—role of Rel/NF-κB in the regulation of apoptosis. Oncogene 2003;22:8961–82.

Laferge-Frayssinet C, Chakor K, Lafont P, et al. Transplacental transfer of T2-toxin: pathological effect. J Environ Pathol Toxicol Oncol 1990;10:64–8.

Leppä S, Bohmann D. Diverse function of JNK signaling and c-Jun in stress response and apoptosis. Oncogene 1999;18:6158–62.

Lühe A, Hildebrand H, Bach U, et al. A new approach to studying ochratoxin A (OTA)-induced nephrotoxicity: expression profiling in vivo and in vitro employing cDNA microarrays. Toxicol Sci 2003;73:315–28.

Marasas WFO, Bamburg JR, Smalley EB, et al. Toxic effects on trout, rats, and mice of T-2 toxin produced by the

fungus *Fusarium tricinctum* (Cd.) Snyd. Et Hans. Toxicol Appl Pharmacol 1969;15:471–82.

Martin LJ, Morse JD, Anthony A. Quantitative cytophotometric analysis of brain neuronal RNA and protein changes in acute T-2 mycotoxin poisoned rats. Toxicon 1986;24:933–41.

Mercurio F, Manning AM. NF-κB as a primary regulator of the stress response. Oncogene 1999;18:6163–71.

Middlebrook JL, Leatherman DL. Binding of T-2 toxin to eukaryotic cell ribosomes. Biochem Pharmacol 1989;38: 3103–10.

Nagase M, Alam MM, Tsushima A, et al. Apoptosis induction by T-2 toxin: activation of caspase-9, caspase-3, and DFF-40/CAD through cytosolic release of cytochrome c in HL-60 cells. Biosci Biotech Biochem 2001;65:1741–7.

Pang VF, Lorenzana RM, Beasley VR, et al. Experimental T-2 toxicosis in swine. III. Morphologic changes following intravascular administration of T-2 toxin. Fundam Appl Toxicol 1987;8:298–309.

Rousseaux CG, Schiefer HB. Maternal toxicity, embryolethality and abnormal fetal development in CD-1 mice following one oral dose of T-2 toxin. J Appl Toxicol 1987;7:281–8.

Ryan KM, Ernst MK, Rice NR, et al. Role of NF-κB in p53-mediated programmed cell death. Nature 2000;404:892–7.

Sánchez-Pérez I, Benitah SA, Martínez-Gomariz M, et al. Cell stress and MEKK1-mediated c-Jun activation modulate NFκB activity and cell viability. Mol Biol Cell 2002;13:2933–45.

Sehata S, Teranishi M, Atsumi F, et al. T-2 toxin-induced morphological changes in pregnant rats. J Toxicol Pathol 2003;16:59–65.

Sehata S, Kiyosawa N, Sakuma K, et al. Gene expression profiles in pregnant rats treated with T-2 toxin. Exp Toxic Pathol 2004;55:357–66.

Shinozuka J, Suzuki M, Noguchi N, et al. T-2 toxin-induced apoptosis in hematopoietic tissues of mice. Toxicol Pathol 1998;26:674–81.

Stanford GK, Hood RD, Hayes AW. Effect of prenatal administration of T-2 toxin to mice. Res Commun Chem Pathol Pharmacol 1975;10:743–6.

Sugamata M, Hattori T, Ihara T, et al. Fine structural changes and apoptotic cell death by T-2 mycotoxin. J Toxicol Sci 1998;23(Suppl. II):148–54.

Thompson WL, Wannemacher Jr. RW. In vivo effects of T-2 mycotoxin on synthesis of proteins and DNA in rat tissues. Toxicol Appl Pharmacol 1990;105:483–91.

Wang J, Fitzpatrick DW, Wilson JR. Effects of the trichothecene mycotoxin T-2 toxin on neurotransmitters and metabolites in discrete areas of the rat brain. Food Chem Toxicol 1998;36:947–53.

World Health Organization (WHO). Selected mycotoxins: ochratoxins, trichothecenes, ergot. Environmental health criteria, vol. 105. Geneva: WHO; 1990.

Yang GH, Jarvis BB, Chung YJ, et al. Apoptosis induction by the satratoxins and other trichothecene mycotoxins: relationship to ERK, p38 MAPK, and SAPK/JNK activation. Toxicol Appl Pharmacol 2000;164:149–60.

Yang MCK, Ruan QG, Yang JJ, et al. A statistical method for flagging weak spots improves normalization and ratio estimates in microarrays. Physiol Genomics 2001;7:45–53.

Available online at www.sciencedirect.com
SCIENCE DIRECT®
Experimental and Toxicologic Pathology 56 (2005) 333–339
EXPERIMENTAL AND TOXICOLOGIC PATHOLOGY
www.elsevier.de/etp

Nitrofurazone-induced gene expressions in rat hepatocytes and their modification by *N*-acetylcysteine

Kyoko Ito[a,*], Satoru Kajikawa[a], Aisuke Nii[a], Kunio Doi[b]

[a]*Safety Research Laboratories, Yamanouchi Pharmaceutical Co., Ltd., 1-8 Azusawa 1-Chome, Itabashi-ku, Tokyo 174-8511, Japan*
[b]*Department of Veterinary Pathology, Faculty of Agriculture, The University of Tokyo, Tokyo, Japan*

Received 31 August 2004; accepted 22 November 2004

Abstract

The antibiotic nitrofurazone (NF) at a subtoxic dose has been shown to increase hepatocyte DNA synthesis with no preceding cell damage or necrosis. This was suppressed by concomitant administration of the antioxidant *N*-acetylcysteine (NAC), which suggests that free radical production is involved in the process. In this study, male F344 rats were given a single oral subtoxic dose of NF to investigate the changes in genes implicated in hepatocyte proliferation between 1 and 20 h postdose by real-time PCR. Some rats were also given NAC to examine the involvement of free radicals. There were transient and sequential increases in mRNA levels of c-myc and c-jun shortly after the administration, followed by tumor necrosis factor-α (TNF-α), transforming growth factor-α (TGF-α), c-Ha-ras, and cyclin E. The increases were blocked by concomitant administration of NAC. In contrast, there were no NF-specific increases in c-fos, hepatocyte growth factor, epidermal growth factor or cyclin D1 mRNAs. These results indicate that the induction of hepatocyte proliferation by NF is triggered by free radicals, with a pathway involving increases in c-jun, c-myc, TNF-α, TGF-α, c-Ha-ras, and cyclin E. The results also indicate that NF-induced proliferation resembles that of other mitogens.

Keywords: Nitrofurazone; Rat; Hepatocyte; Gene expression; Proliferation; *N*-acetylcysteine; c-fos; c-myc; c-jun; c-Ha-ras; Tumor necrosis factor-α (TNF-α); Transforming growth factor-α (TGF-α); Hepatocyte growth factor (HGF); Epidermal growth factor (EGF); cyclin D1; cyclin E

Introduction

Nitrofurazone (5-nitro-2-furaldehyde semicarbazone; NF), a broad-spectrum antibiotic, has been known to elicit toxic effects, including convulsive seizures, testicular degeneration, and degenerative arthropathy in rodents (Hagenäs et al., 1978; Kari et al., 1989). It has, in addition, been reported to induce necrotic changes in the liver and adrenal gland at high doses (Ito et al., 2004). In contrast, NF at low doses elicits hepatocyte proliferation without the preceding loss of hepatocytes, i.e. it acts as a mitogen (Ito et al., 2002). Indeed, in mice fed NF for 13 weeks, liver to body weight ratios were moderately increased (Kari et al., 1989), apparently without histopathological changes. The mitogenic effect is abrogated by concomitant administration of antioxidants *N*-acetylcysteine (NAC) or cyanidanol, indicating the involvement of free radical production (Ito et al., 2003). It is noteworthy that NF behaves as a

*Corresponding author.
E-mail address: itou@yamanouchi.co.jp (K. Ito).

0940-2993/$ - see front matter © 2005 Elsevier GmbH. All rights reserved.
doi:10.1016/j.etp.2004.11.002

hepatotoxicant at higher doses and as a mitogen at lower, subtoxic doses. Such is also the case with agents which are generally better known for hepatotoxicity such as thioacetamide (Mangipudy et al., 1995a, b) and carbon tetrachloride (CCl_4, Rao et al., 1997).

Proliferation of hepatocytes occurs very infrequently in normal adult rodents, the vast majority of cells being in the resting phase of the cell cycle (G_0). Hepatocytes, however, are equipped with mechanisms which allow them to quickly modulate the rate should the need arise. Two different types of proliferation are currently known, compensatory proliferation and mitogen-induced proliferation (Ledda-Columbano et al., 1993; Columbano and Shinozuka, 1996). Compensatory proliferation follows the loss of hepatocytes after partial hepatectomy or "chemical hepatectomy" by hepatotoxicants such as CCl_4. Mitogen-induced proliferation, in contrast, entails no overt damage or loss of hepatocytes. "Mitogens" include a broad spectrum of chemically unrelated substances such as lead nitrate (Columbano et al., 1983), cyproterone acetate (CPA, Roberts et al., 1995), cyclosporine (Masuhara et al., 1993), ethylene dibromide (EDB, Nachtomi and Farber, 1978), and hypolipidemic drugs (e.g. Wy-14,643, Rusyn et al., 2000), as well as a large number of stimuli. These include free radicals, decreases in protective enzymes, glutathione depletion, and sustained accumulation of normally low endogenous products (Iatropoulos and Williams, 1996). Although the two modes of proliferation share some of the events following the trigger, there are also differences in the series of changes in growth factors and early response genes. Compensatory proliferation involves increases in hepatocyte growth factor (HGF), transforming growth factor-α (TGF-α), epidermal growth factor (EGF), tumor necrosis factor-α (TNF-α), c-fos, c-myc, c-jun, and c-Ha-ras (Fausto and Mead, 1989; Fausto et al., 1995; Fausto, 1996), whereas some of these are unaltered in mitogen-induced proliferation (Coni et al., 1990, 1993; Masuhara et al., 1993; Goldsworthy et al., 1994; Shinozuka et al., 1994).

Much attention has recently been devoted to the mechanism involving free radicals. Free radicals at high concentrations inflict damage on cells, but at low doses are believed to act as a mediator of various signaling pathways within a cell (Remacle et al., 1995). The antioxidant NAC is widely used as an experimental tool in biological and pathological processes. Its mode of action is two-fold, as a free radical scavenger by directly reacting with them, and, additionally, it elevates intracellular glutathione content by providing a precursor (Zafarullah et al., 2003), thereby enhancing the cellular defense system. It has been used to counteract the effects of free radicals, and the mitogenic effect of NF has been prevented by its concomitant administration (Ito et al., 2003), suggesting the involvement of free radicals in the process.

This study examines the changes in gene expressions generally associated with hepatocyte proliferation in order to further characterize the nature of NF's mitogenic effect. The effect of NAC, which blocks free radicals and NF-induced proliferation, was concurrently examined for the modification of NF-induced genes in an attempt to elucidate to what extent free radicals contribute to the sequence of events following the use of NF.

Materials and methods

Animals

SPF male Fischer rats were purchased from Charles River Japan Inc. (Kanagawa, Japan), and acclimated until use in a room which was kept at 23±2 °C, with a relative humidity of 55±10%, ventilated 15 times/h, and lighted for 13 h (from 8:00 a.m. to 9:00 p.m.). The animals were given a commercially available diet (CRF-1, Oriental Yeast Co., Ltd., Tokyo, Japan) and tap water ad libitum. The rats were 10–11 weeks old at the start of treatment. All animals received humane care throughout the experiment in compliance with the institutional guidelines for the care and use of laboratory animals.

Nitrofurazone and *N*-acetylcysteine administration and sample collection

NF (Wako Pure Chemical Industries, Ltd., Osaka, Japan) was suspended at a concentration of 16 mg/mL in a 0.5% methylcellulose solution. NAC (Wako Pure Chemical Industries, Ltd.) was dissolved in saline at a concentration of 20 mg/mL.

Rats were given a single dose of NF at 80 mg/kg (5 mL/kg) by gavage using a stomach tube. Five animals were sacrificed at 1, 2, 5, 8, 12, 16, and 20 h postdose, respectively (NF rats). In addition, five rats each were given an intraperitoneal injection of NAC at 50 mg/kg (2.5 mL/kg) 30 min before and, where applicable, 5 h after NF administration, and sacrificed as above (NAC + NF rats). Five rats given a 0.5% methylcellulose solution alone served as controls at each time point.

Rats were sacrificed by exsanguination under ether anesthesia. The liver was excised for total RNA extraction.

RNA extraction and reverse transcription

The liver was homogenized in approximately 1 mL of ISOGEN (Nippon Gene, Tokyo, Japan) per 100 mg of tissue, and total RNA was extracted according to the manufacture's instructions. Total RNA was quantified

using a spectrophotometer set at a 260-nm wavelength. Contaminating DNA was removed from the RNA samples during a 15-min digestion at room temperature with DNase I, Amplification Grade (Invitrogen Corporation, Carlsbad, CA, USA). Total RNA (0.8 μg) from each sample was converted to cDNA at a final volume of 20 μl using Super Script First-Strand Synthesis System for RT-PCR (Invitrogen Corporation) as instructed by the manufacturer. A thermal cycler GeneAmp PCR System 9600 (Applied Biosystems, Foster City, CA, USA) was used. The cDNA was then diluted and used in subsequent PCR reactions

Real-time PCR

A length of the target gene was amplified in a mixture of water, cDNA, primer pair, and SYBR® Green PCR Master Mix (Applied Biosystems) using an ABI Prism 7700 or 7900 HT (Applied Biosystems). The final concentration of the primers was 200 nM each. The number of cycles was between 40 and 48, and the annealing temperature was between 58 and 60 °C. The sequences of the primers used for each of the genes analyzed are described in Table 1. Primers for glyceraldehyde-3-phosphate dehydrogenase (GAPDH) were from Taqman® Rodent GAPDH Control Reagents (Applied Biosystems) with a product size of 177 bp. Electrophoretic analysis of expected product sizes was performed for all primer sets prior to real-time RT-PCR to confirm the fidelity of the reaction. The standard curves were generated using a dilution series of corresponding purified PCR products. The data were processed using a Sequence Detection System (Applied Biosystems). A housekeeping gene, GAPDH, was used for normalizing the amount of each sample. The data were analyzed statistically with the Student's *t*-test to compare treated groups with the control, expressed as mean ± standard error (SE), and illustrated as a ratio to the control.

Results and discussion

Fig. 1a illustrates changes in c-jun mRNA levels between 1 and 8 h postdose in control, NF, and NAC+NF rats. The expression of c-jun was increased at 1 and 2 h in NF rats with a higher peak at 1 h. Similarly, c-myc was increased significantly in NF rats during both hours, but experienced a peak at 2 h (Fig. 1b). No increase in c-fos was specific to NF rats (data not shown). Another protooncogene, c-Ha-ras, was increased in NF rats at a later phase, between 8 and 12 h (Fig. 1c). The increases in protooncogenes c-jun, c-myc, and c-Ha-ras were partially or completely abolished in NAC+NF rats, indicating the NAC inhibited the effect of NF in enhancing the expression of these genes. TNF-α in NF rats was increased from 2 to 8 h, but decreased to the control level at 12 h (Fig. 1d). Changes in TGF-α between 5 and 16 h are shown in Fig. 1e. The expression was highest at 8 h and higher, but statistically insignificant at 12 h. Cyclin E was slightly increased in NF rats at 16 h, and further at 20 h (Fig. 1f). Again, increases in these genes after NF administration were suppressed by concomitant administration of NAC. An apparent increase in cyclin E was seen at 8 h in NF rats, but so was in NAC+NF rats; these are therefore likely to be biologically insignificant, together with the fact that there was no incorporation of BrdU at 12 h in a pilot study which should follow cyclin E expression. The increases, in sequential order, were in: c-jun, c-myc, TNF-α, TGF-α, c-Ha-ras, and cyclin E. There was no NF-specific increase in HGF, EGF or cyclin D1 expression (data not shown).

The results of the current study are strikingly similar to other mitogenic substances in the set of genes increased and those unaltered. Of the two proliferation modes, compensatory proliferation involves increases in growth factors including HGF, TGF-α, EGF, and TNF-α, and protooncogenes such as c-fos, c-myc, c-jun, and c-Ha-ras (Fausto and Mead, 1989; Fausto et al., 1995; Fausto, 1996). In contrast, although differences exist, mitogens are often associated with increases in c-jun,

Table 1. Oligonucleotide sequences of PCR primers

Gene	Size (bp)	Forward	Reverse
c-myc	106	AGG AGA AAC GAG CTG AAG CGT A	CGG TGG CTT TTT TGA GGA TAA CT
c-jun	64	GAA AAC CTT GAA AGC GCA AAA C	CAC CTG TTC CCT GAG CAT GTT
c-fos	136	GAA GGG AAA GGA ATA AGA TGG CT	TTC AGT AGA TTG GCA ATC TCG G
c-Ha-ras	97	CTG GAC ATC TTA GAC ACA GCA GG	TGA TGG CAA ATA CAC AGA GGA AG
TNF-α	141	GTG ATC GGT CCC AAC AAG GA	TGC TTG GTG GTT TGC TAC GA
TGF-α	170	TGG GTC AAG GCC AAG TGT	TAT CAT CGG AAG CTA ACG GTG
HGF	83	CAA AAC AAG GTC TGG ACT CAC ATG	CGT CTG GCT CCC AGA AGA TAT G
EGF	218	TCA CTG GGA AAG ACT GCA AGA A	AGA TAC ACT GCA AGT GTG GCC C
Cyclin D1	86	CCG TCC ATG CGG AAG ATC	ATG GCC AGC GGG AAG AC
Cyclin E	149	GTG AAA AGC CAG GAT AGC AGT CA	CTG GGC GGT CTG ATT TTC C

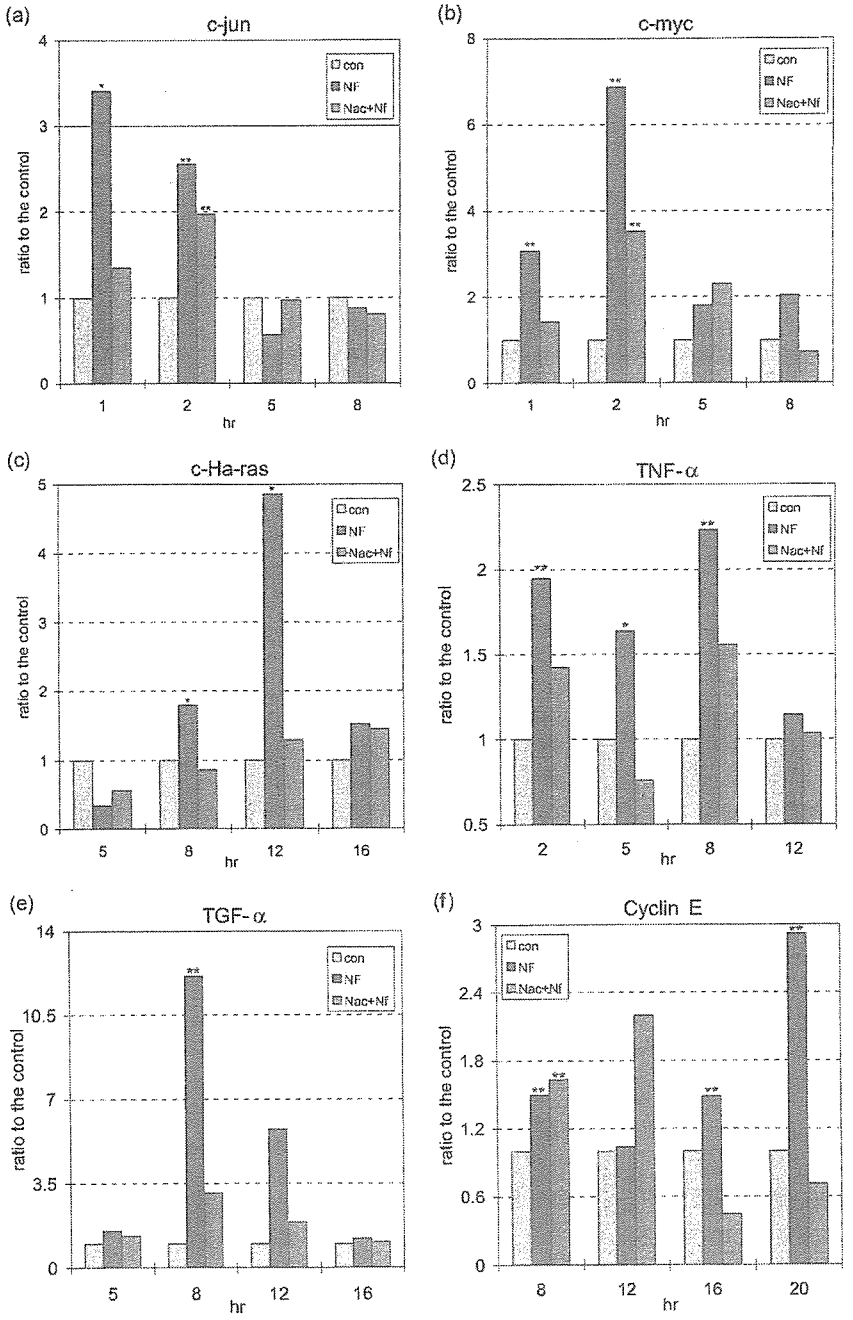

Fig. 1. (a) c-jun, (b) c-myc, (c) c-Ha-ras, (d) TNF-α, (e) TGF-α, and (f) cyclin E expression, respectively, following NF or NAC+NF treatment, and expressed as a ratio to the control. $^{*}P<0.05$ and $^{**}P<0.01$.

c-myc, and TNF-α; increases in c-fos and HGF, however, are often absent (Coni et al., 1993; Goldsworthy et al., 1994; Masuhara et al., 1993; Shinozuka et al., 1994). In the present study, c-jun, c-myc, and TNF-α were increased in NF rats, and suppressed in NAC+NF rats. HGF and c-fos were not predictive of NF-induced hepatocyte proliferation. To what extent these NF-induced genes are involved in hepatocyte proliferation is unclear at this stage, but the fact that these genes were suppressed when hepatocyte proliferation was inhibited by NAC supports the notion that they are collectively responsible for NF-induced proliferation.

The majority of adult hepatocytes under normal circumstances are in the quiescent phase (G_0), but they re-enter the cell cycle in response to a proliferative stimulus. Hepatocytes undergo the process of "priming"

during this step, which renders the cells capable of responding to a further proliferative stimulus by going through a $G_0 \rightarrow G_1$ transition (Webber et al., 1994). Hepatocytes need both priming and growth stimuli for passing through the "restriction point" to enter the S phase. A one-third hepatectomy increases c-myc, but does not induce DNA synthesis (Webber et al., 1994). A single injection of HGF in normal rats induces no or only limited hepatocyte proliferation (Webber et al., 1994). In contrast, infusion of HGF or TGF-α to 30% hepatectomized rats resulted in significant increases in DNA synthesis (Webber et al., 1994). In the present study, increases in c-myc and possibly another proto-oncogene, c-jun, in NF-treated rats may have worked in the priming step, even though these genes may not have induced proliferation per se. In this context, it is of interest that the second administration of NF to rats induced a greater increase in DNA synthesis than the first dose (Ito et al., 2002). A larger portion of hepatocytes may have entered the cell cycle upon the second administration because of the priming by the first dose. A similar phenomenon is also known: in auto- and heteroprotection, a small dose of a chemical protects against a second lethal dose of the same or another compound, respectively (Chanda et al., 1995; Mangipudy et al., 1995a; Soni and Mehendale, 1998). It is considered that the smaller dose primes hepatocytes and enables them to proliferate more efficiently in an attempt to compensate for cell loss by necrosis.

The increase in TGF-α was unexpected since it is often unaltered by mitogens (Masuhara et al., 1993; Shinozuka et al., 1994). TGF-α is stimulated by HGF, and these are often expressed in concert. The expressions of both these genes are increased following partial hepatectomy, and, in contrast, are often suppressed in mitogen-induced proliferation. TGF-α is, however, thought to be more closely correlated with hepatocyte proliferation than HGF (Tomiya et al., 1998). TGF-α is also known to be directly up-regulated by TNF-α (Gallucci et al., 2000). There was no NF-specific increase in HGF in this study, whereas both TNF-α and TGF-α were increased. The increases in both these factors were seen at similar hours, but the elevation of TGF-α persisted longer than that of TNF-α. It is conceivable that TGF-α was induced by TNF-α, although other possibilities cannot be excluded.

The expression of c-Ha-ras was increased in NF rats between 8 and 12 h, later than other protooncogenes such as c-jun and c-myc. It is interesting that a similar pattern of increase in c-Ha-ras is seen with other mitogens including CPA and EDB, as well as in compensatory proliferation following partial hepatectomy and CCl_4 (Coni et al., 1990). The increase in c-Ha-ras expression is said to coincide with the increase in DNA synthesis and mitosis in these experiments. On the other hand, Ras activity functions late in G_1 phase and is required for passage through the restriction point, and entry into the S phase in growth factor-stimulated fibroblasts (Takuwa and Takuwa, 1997). No increase in DNA synthesis was seen in the hepatocytes of NF rats at 12 h postdose in a pilot study, the time when c-Ha-ras was increased. An increase in cyclin E followed that in c-Ha-ras. It is, therefore, more likely that c-Ha-ras is associated with the entry into the S phase in this experiment, rather than coinciding with DNA synthesis.

Cyclin D1, along with cyclin E, is said to be another critical protein in the G_1 phase, acting generally in sequence. Cyclin E is the major downstream target of cyclin D1. Contrary to our expectations, no increase in cyclin D1 was seen in parallel to, or slightly previous to, cyclin E expression in NF-treated rats. It is suggested that the roles of cyclin D1 can be bypassed and that cyclin E is more involved in directly activating the downstream events of G_1 progression or S phase entry (Roberts, 1999). Studies in other systems indicate that the activation of the cyclin E system is sufficient to trigger cell cycle progression in the absence of cyclin D1 (Connell-Crowley et al., 1998). Also compatible with this idea is that the replacement of cyclin D1 with cyclin E can completely rescue the developmental defects observed in cyclin D1-deficient animals (Sherr and Roberts, 1999). These facts suggest that, although the possibility of posttranscriptional activation of cyclin D1 cannot be excluded, NF-induced hepatocyte proliferation may possibly be mediated by a pathway involving cyclin E, without cyclin D1 participation.

The hypothetical sequence of events associated with NF-induced hepatocyte proliferation can be summarized as in Fig. 2. It is accepted that free radicals within the cell's antioxidant capacity induce cell growth (Remacle et al., 1995). As mentioned above, the involvement of free radicals is implicated in NF-induced proliferation, which is suppressed by antioxidants. Various genes were increased following NF, but those that are inhibited by NAC are likely to play more critical roles in the process: c-jun, c-myc, TNF-α, TGF-α, c-Ha-ras, and cyclin E. Free radical generation during NF metabolism (Tatsumi et al., 1976; Peterson et al., 1979; Wolpert et al., 1973) is likely to rise almost immediately after administration, since the blood plasma concentration of NF peaks at 1 h postdose (Ito et al., 2002). Free radicals produced during NF metabolism may lead to increases in immediate early genes such as c-jun and c-myc, resulting in the priming of hepatocytes which have now acquired competence for cell growth. These events are followed by proliferative stimulation by TNF-α, or TGF-α, or both. The expression of c-Ha-ras, in concert with other genes including cyclin E, conceivably allow hepatocytes to pass through the restriction point and enter the S phase of the cell cycle, finally culminating in DNA synthesis. What is still unclear is the precise mechanism through which NAC suppresses NF-induced proliferation in hepatocytes. It remains to